



Identifying Better Indicators of Aerosol Wet Scavenging During Long-Range Transport

Miguel Ricardo A. Hilario¹, Avelino F. Arellano¹, Ali Behrangi^{1,2}, Ewan C. Crosbie^{3,4}, Joshua P. DiGangi³, Glenn S. Diskin³, Michael A. Shook³, Luke D. Ziemba³, and Armin Sorooshian^{1,5}

5 ¹ Department of Hydrology and Atmospheric Sciences, University of Arizona, Tucson, AZ, USA

² Department of Geosciences, University of Arizona, Tucson, AZ, USA

³ NASA Langley Research Center, Hampton, VA, USA

⁴ Science Systems and Applications, Inc., Hampton, VA, USA

⁵ Department of Chemical and Environmental Engineering, University of Arizona, Tucson, AZ, USA

10 *Correspondence to:* Armin Sorooshian (armin@arizona.edu)

Abstract. As the dominant sink of aerosol particles, wet scavenging greatly influences aerosol lifetime and interactions with clouds, precipitation, and radiation. However, wet scavenging remains highly uncertain in models, hindering accurate predictions of aerosol spatiotemporal distributions and downstream interactions. In this study, we present a flexible, computationally inexpensive method to identify meteorological variables relevant to estimating wet scavenging using a combination of aircraft, satellite, and reanalysis data augmented by trajectory modeling to account for air mass history. Treating the enhancement (Δ) ratio of black carbon and carbon monoxide ($\Delta BC/\Delta CO$) measured by aircraft as an in situ proxy for wet scavenging, we assess the capabilities of an array of meteorological variables to predict $\Delta BC/\Delta CO$ using regression statistics derived from curve-fitting and k-fold cross-validation. We find that accumulated precipitation along trajectories (APT) – treated as a wet scavenging indicator across multiple studies – is unable to accurately capture $\Delta BC/\Delta CO$ trends, suggesting that APT is not a good indicator of wet scavenging effects. In contrast, the frequencies of precipitation or high relative humidity along trajectories better predict $\Delta BC/\Delta CO$ trends and magnitudes, suggesting that these types of meteorological variables are better than APT for estimating the degree of wet scavenging in an air mass. Precipitation characteristics (e.g., intensity, frequency) from satellite retrievals are better indicators of $\Delta BC/\Delta CO$ than those calculated from reanalysis, supporting previous studies that demonstrated reanalysis to be less reliable than satellite retrievals in terms of precipitation. Finally, top quantiles (e.g., 90th) of relative humidity are able to consistently capture the behavior of $\Delta BC/\Delta CO$ and may also be a more suitable indicator of wet scavenging than APT. Future studies can use the best-performing meteorological variables identified in our study to estimate wet scavenging. Furthermore, this method can be repeated for different regions to identify region-specific factors influencing wet scavenging, and our findings may be useful for informing scavenging parametrization schemes in models.



30 1 Introduction

Although wet scavenging is the dominant removal mechanism for atmospheric aerosol particles (Seinfeld and Pandis, 2016; Textor et al., 2006), it remains a large source of uncertainty in global-scale models (Watson-Parris et al., 2019; Liu and Matsui, 2021; Moteki et al., 2019; Hodzic et al., 2016). This uncertainty hampers the ability of global-scale models to capture the lifecycle (i.e., sources, transformations, and sinks) (Hou et al., 2018), spatial extent (Moteki et al., 2019), and vertical profile (Watson-Parris et al., 2019; Liu and Matsui, 2021; Frey et al., 2021; Kipling et al., 2016) of aerosol particles. Inaccurate representations of these aerosol features contribute to uncertainties in estimates of aerosol radiative effects (Samset et al., 2013; Marinescu et al., 2017) and aerosol loadings over climate-sensitive regions (Liu and Matsui, 2021; Mahmood et al., 2016; Shen et al., 2017), with further implications for the remote sensing of aerosol abundance downwind of precipitating or cloudy areas. Advancing knowledge of wet scavenging processes can help reduce the largest uncertainty in human forcing of the climate system, which involves aerosol-cloud interactions (e.g., Bellouin et al., 2020).

Wet scavenging occurs either below- or in-cloud. Below-cloud scavenging occurs when aerosol particles are collected by precipitation (Croft et al., 2009) and is most important between the surface and 1 km above ground level (AGL) (Grythe et al., 2017). The efficiency of below-cloud scavenging depends on raindrop size distributions and aerosol composition (Lu and Fung, 2018; Grythe et al., 2017) as well as the amount of in-cloud condensed water (Luo et al., 2019). To calculate the fraction of aerosol scavenged below-cloud, models typically rely on an empirically-derived below-cloud scavenging coefficient, which is a function of aerosol size (Feng, 2007; Croft et al., 2009) and composition (Lin et al., 2021). Semi-empirical model parametrizations of below-cloud scavenging have been shown to improve simulated surface concentrations (Luo et al., 2019); however, agreement between models and observations is highly sensitive to the specific below-cloud scavenging scheme used (Lu and Fung, 2018). Below-cloud scavenging rates in models also remain significantly underestimated compared to observations (Kim et al., 2021; Ryu and Min, 2022; Xu et al., 2019).

In-cloud scavenging occurs via nucleation (i.e., activation of aerosol particles into cloud droplets; Jensen and Charlson, 1984) or impaction (i.e., collision of interstitial aerosol particles with existing cloud droplets; Kipling et al., 2016; Flossmann et al., 1985) and is followed either by (1) precipitation that reaches the surface, removing the particle from the atmosphere (Radke et al., 1980), or (2) evaporation of cloud droplets or precipitation, returning the scavenged particle to the free atmosphere (Mitra et al., 1992). Model improvements in in-cloud scavenging include using a continuous rather than binary cloud fraction (Ryu and Min, 2022; Xu and Randall, 1996), accounting for cloud water phase (Grythe et al., 2017; Liu and Matsui, 2021), and accurately simulating cloud supersaturation (Moteki et al., 2019). Although in-cloud scavenging is generally thought to be more efficient at removing accumulation mode aerosol particles (Watson-Parris et al., 2019; Choi et al., 2020), other studies argue that there are instances wherein below-cloud scavenging becomes more important at regulating aerosol burdens (Kim et al., 2021; Ryu and Min, 2022; Xu et al., 2019). Uncertainties related to wet scavenging are further exacerbated by the divergent role of clouds, which can be a sink or source of aerosol particles depending on environmental factors and cloud characteristics (Ryu et al., 2022).

One avenue for improving the estimation of wet scavenging, particularly in observational studies, is to identify an effective indicator of wet scavenging. Previous studies used precipitation amount (Feng, 2007; Andronache, 2003) while more recent studies accounted for air mass history using the National Oceanic and Atmospheric Administration (NOAA) Hybrid Single Particle Lagrangian Integrated Trajectory Model (Rolph et al., 2017; Stein et al., 2015) to calculate accumulated precipitation along trajectories (APT) (e.g., Kanaya et al., 2016, 2020). However, APT can be problematic as an indicator of wet scavenging because APT is an accumulated quantity and does not consider specific characteristics of precipitation relevant to scavenging such as intensity and frequency (Hou et al., 2018; Wang et al., 2021c, b; Hilario et al., 2022). APT as an indicator of wet scavenging also



70 relies on the correct detection of precipitation and retrievals of amounts, which are challenging during both light (Nadeem et al.,
2022; Kidd et al., 2021) and intense precipitation events (Chen et al., 2020a; Gupta et al., 2020) and even show disagreements
between different satellite precipitation products (SPPs) and reanalyses (Cannon et al., 2017; Jiang et al., 2021; Alexander et al.,
2020; Chen et al., 2020b; Barrett et al., 2020). Furthermore, precipitation from SPPs such as the Precipitation Estimation from
Remotely Sensed Information using Artificial Neural Networks – Climate Data Record (PERSIANN-CDR) (Ashouri et al., 2015;
Nguyen et al., 2018) and the Integrated Multi-satellitE Retrievals for the Global Precipitation Measurement (GPM) mission
75 (IMERG) (Huffman et al., 2020) refer to total column precipitation that have been validated mainly with surface measurements
(Sapiano and Arkin, 2009; Nicholson et al., 2019; Wang et al., 2021a) and consequently may not detect precipitation that evaporates
before reaching the surface (e.g., virga) (Wang et al., 2018).

Given the uncertainties of estimating wet scavenging from precipitation, we present a flexible, computationally inexpensive
method to identify alternative meteorological variables that can be used to better estimate wet scavenging. We combine curve-
fitting and k-fold cross-validation to evaluate an array of meteorological variables from aircraft, satellite, and reanalysis data to
80 answer the following:

- (1) What meteorological variables can estimate wet scavenging trends better than APT? Since precipitation frequency has
been shown to exert significant control over aerosol scavenging (Wang et al., 2021b), we hypothesize that predictors that
account for the frequency of scavenging-conducive conditions (e.g., frequency of high relative humidity (RH) conditions
85 along trajectories) will be able to capture wet scavenging trends better than APT.
- (2) How can APT be filtered or changed to better estimate wet scavenging? We hypothesize that considering precipitation
intensity and/or trajectory altitude thresholds when calculating APT will improve its ability to estimate wet scavenging.
We also hypothesize that calculating APT using SPPs will perform better than APT from reanalysis.

The presented method may be repeated over different regions to identify region-specific wet scavenging indicators. This can
90 inform scavenging parameterization development for models by providing guidance on what meteorological variables are needed
to properly capture wet scavenging processes over a specific region. Future studies can also use the best-performing variables
identified in this study as alternatives to APT when estimating the extent of wet scavenging.

2 Data & Methods

2.1 Aircraft data

95 Much of the methodology and instrument details in this study are detailed elsewhere (Hilario et al., 2021) but are summarized
here. We utilize aircraft measurements from NASA's Cloud, Aerosol, and Monsoon Processes-Philippines Experiment
(CAMP²Ex; 24 August to 5 October 2019) over the tropical West Pacific (Reid et al., 2023), which hosts a dynamic transport
environment rich in aerosol sources and cloud-precipitation systems.

100 Black carbon (BC)-equivalent concentrations (particle diameters: 100 – 700 nm) were measured with a Single-Particle Soot
Photometer (SP2) (Moteki & Kondo, 2007, 2010) with an uncertainty of 15% (Slowik et al., 2007) and lower detection limit of 10
ng m⁻³ verified by filter-blank measurements as well as observations in the clean free troposphere. To eliminate in-cloud sampling
artifacts such as droplet shattering on the inlet (Murphy et al., 2004), we use only data collected outside of clouds. All BC
concentrations are reported at standard temperature and pressure (273 K, 1013 hPa). Carbon monoxide (ppm) was measured using
a dried-airstream near-infrared cavity ringdown absorption spectrometer (G2401-m; PICARRO, Inc.), with an uncertainty of 2%
105 and precision of 0.005 ppm. As an in situ (i.e., at the aircraft's position) contrast to moisture-based variables along trajectories,



relative humidity ($RH_{w,DLH}$) was derived from absolute water vapor concentrations that were retrieved by a diode laser hygrometer (DLH) (Livingston et al., 2008) on the aircraft.

2.2 Enhancement ratio calculation

To relate wet scavenging to transport conditions, previous studies used enhancement (Δ) ratios of BC and carbon monoxide (CO) ($\Delta BC/\Delta CO$; Hilario et al., 2021; Kanaya et al., 2016; Oshima et al., 2012). By using the enhancement above background, $\Delta BC/\Delta CO$ accounts for spatial variations in the background levels of BC and CO and is better able to detect an air mass containing BC and CO above background levels. This ratio can be used as an indicator of wet scavenging because BC is relatively chemically inert and is mainly removed from the atmosphere via wet scavenging (Moteki et al., 2012). While CO is also relatively chemically inert, CO has a lifetime between 30 to 90 days (Seinfeld and Pandis, 2016) that is mainly controlled by photochemistry rather than wet scavenging due to its low solubility. Because of this, we use $\Delta BC/\Delta CO$ as our proxy for wet scavenging and the predictand for our regression models.

Enhancements were defined as the difference between species concentrations and the lowest 5th percentile species concentration for all CAMP²Ex data for every 5 K potential temperature bin (Koike et al., 2003; Matsui et al., 2011). As CAMP²Ex spanned the late southwest monsoon and early monsoon transition, background concentrations (i.e., lowest 5th percentile) were calculated for each monsoon phase using 20 September 2019 to divide the two monsoon phases. Only data with $\Delta CO > 0.02$ ppm were included to reduce uncertainties caused by low denominator values in the $\Delta BC/\Delta CO$ ratio (Kleinman et al., 2007; Kondo et al., 2011; Matsui et al., 2011).

2.3 Trajectory modeling

Trajectory modeling is a computationally inexpensive tool for characterizing transport processes (Kanaya et al., 2016; Oshima et al., 2012; Moteki et al., 2012) and has been used in synergy with aircraft data (Hilario et al., 2021; Dadashazar et al., 2021). In this study, we use trajectories to account for meteorological conditions during air parcel transport that are expected to impact the scavenged aerosol fraction. Backward trajectories were spawned every minute along the aircraft flight path and run for 72 hours using the NOAA HYSPLIT model. Meteorological input data for the HYSPLIT model were from the National Centers for Environmental Prediction (NCEP) Global Forecast System reanalysis (GFS; $0.25^\circ \times 0.25^\circ$).

2.4 Data for predictor variables

Several meteorological variables (i.e., predictors) considered in this work were calculated from GFS reanalysis collocated along each trajectory. Though reanalysis is relatively coarse and not cloud-resolving, reanalysis variables (e.g., RH) may still be useful in detecting the presence of meso-to-synoptic-scale cloud fields. As precipitation is expected to be accompanied by elevated RH or water vapor mixing ratio (MR), these reanalysis-derived variables could serve as effective scavenging indicators in cases where precipitation may be missed or misestimated.

In addition to APT from GFS, we calculated APT from two SPPs: PERSIANN-CDR ($0.25^\circ \times 0.25^\circ$, daily resolution) (Ashouri et al., 2015; Nguyen et al., 2018) and IMERG Final v6 ($0.1^\circ \times 0.1^\circ$, 30-min resolution) (Huffman et al., 2020). We converted precipitation from these products to hourly amounts to match trajectory timesteps prior to further calculation.

Besides APT, we also calculated precipitation amount (PA; mm h^{-1}), frequency (PF), and intensity (PI; mm h^{-1}), which are well-established in the literature for characterizing precipitation, particularly in diurnal cycle analyses (e.g., Zhang et al., 2017; Hilario et al., 2020). Applying these quantities to precipitation along trajectories, PA is APT divided by the total number of hours along the trajectory (i.e., trajectory length) to obtain an average hourly precipitation rate, PF is the fraction of hours along the



trajectory where the grid cell precipitation is above 0 mm, and PI is the ratio of PA to PF. Table 1 shows notation used to explain each type of predictor and its variations.

145 2.5 Curve-fitting and k-fold cross-validation

To quantify relationships between $\Delta BC/\Delta CO$ and each predictor, we performed k-fold cross-validation ($k = 10$) parallelized using the Python package `jug` (Coelho, 2017). To create k distinct partitions of the data, we utilized stratified random sampling wherein random sampling was performed for every 5th percentile block of the predictor such that the sampling probability better reflects the distribution of predictor values (e.g., precipitation) and the resulting partition captures the behavior of $\Delta BC/\Delta CO$ over the whole range of predictor values. By randomly sampling each percentile block for k distinct partitions, this sampling method improves the chances of capturing intra-block variability in $\Delta BC/\Delta CO$ by collecting the most samples where the most data exist. The random nature of the sampling also allows for the consideration of extreme values in the curve-fitting, with a sampling probability proportional to the frequency of these extreme values. As an example, Fig. 1a shows the emphasis of the stratified random sampling method on high density areas of the scatterplot of RH_{q90} and $\Delta BC/\Delta CO$, denoted by dense percentile blocks. For extremely skewed distributions such as APT, several of the lower-value percentiles exhibited non-unique values (e.g., zero). In the case of repeated percentile values, these percentile-based groups were merged. We imposed a minimum of six distinct percentile blocks to ensure robust curve-fitting.

An iterative train-test split procedure using these partitions was then performed using nine partitions as the training set and the remaining partition as the testing set (Fig. 1a). For each iteration of the k-fold cross-validation, nonlinear least squares curve-fitting was applied to the training set (i.e., 9 partitions), to determine coefficients for the equation (e.g., general exponential; discussed below) fitted onto the scatterplot of $\Delta BC/\Delta CO$ and the predictor. We used these coefficients and the testing set (i.e., the remaining partition) as inputs for the curve-fitting equation and calculated a predicted curve of $\Delta BC/\Delta CO$ and the predictor. To assess this predicted curve, we applied stratified random sampling on the testing set and took the median $\Delta BC/\Delta CO$ per 5th percentile block to create observed curves of $\Delta BC/\Delta CO$ as a function of the predictor that could be compared to the predicted curve (Fig. 1b). Because decreases in $\Delta BC/\Delta CO$ are expected to be mainly from wet scavenging, the overall trend or median curve may be treated as a reasonable indicator of wet scavenging effects on $\Delta BC/\Delta CO$ related to changes in the predictor value.

Using a linear regression of predicted and observed median $\Delta BC/\Delta CO$ per 5th percentile block of the predictor (Fig. 1c), we calculated statistics to describe the performance of the predictor (e.g., slope, R). Note that the performance of a predictor refers to how well $\Delta BC/\Delta CO$ derived from the predictor matches observed $\Delta BC/\Delta CO$. We also computed statistics comparing predicted and observed $\Delta BC/\Delta CO$ for individual points (Fig. 1d) rather than medians to assess how much variability in $\Delta BC/\Delta CO$ is captured by the predicted curves. These individual-point statistics resulted in correlations and slopes further from ideal values compared to the median-based statistics. This is expected as individual $\Delta BC/\Delta CO$ points have high variability due to factors other than wet scavenging; however, a comparison of individual-point and median-based statistics show that they qualitatively agree quite well, with the relative ranking of predictors largely unchanged between the two types of statistics. In other words, the top predictors performed well whether we used median-based or individual-point statistics, implying the conclusions reached using our method are qualitatively unaffected. For simplicity, reported statistics in this study refer to median-based statistics unless otherwise specified.

To determine if a predicted $\Delta BC/\Delta CO$ curve tended to overestimate or underestimate observed $\Delta BC/\Delta CO$, we calculated a weighted area difference (WAD) using Eq. 1:

$$180 \quad WAD = \frac{\sum N_i \cdot x_i}{\sum N_i} \quad (1)$$

5



where x_i is the difference between observed and predicted $\Delta BC/\Delta CO$ for the i^{th} percentile block and N_i is the number of data points in that percentile block. A positive (negative) WAD indicates an overestimate (underestimate) of observed $\Delta BC/\Delta CO$.

To account for differing relationships between $\Delta BC/\Delta CO$ and each predictor, we fitted their scatterplot using multiple nonlinear equations (Table 2) and chose the equation producing the highest Pearson correlation (R) between observed and predicted $\Delta BC/\Delta CO$ for that predictor. We use R because we are more interested in predictors that can capture trends in $\Delta BC/\Delta CO$ rather than magnitudes. For some combinations of predictors and curve-fitting equations, the curve-fitting did not successfully converge (< 4% of all combinations and k-fold iterations). In these cases, we did not include the predictor-equation combination in our analysis. However, curve-fitting on the predictor may still converge when using a different equation. In such a scenario, the predictor becomes part of our analysis.

This procedure was repeated for k iterations using a different partition for the testing set in each iteration, which provides a measure of uncertainty in the resulting regression statistics. Sensitivity testing with the k value showed no significant effect on the general conclusions of the study.

Although there is no physical process built into this procedure, the strength of the method is its repeatability in different environments or regions with minimal changes to the overall procedure. As it requires no physical model to be run besides the trajectory calculations, the method is also relatively computationally inexpensive. Future work wanting a more physical basis may apply our method as a diagnostic tool to identify and narrow down a list of meteorological variables that may be relevant to wet scavenging and continue their analysis with a physical model using the narrowed list of variables to analyze.

3 Results and Discussion

3.1 Overall statistical performance

Figures 2-3 show performance comparisons of different predictors derived from linear regressions of observed and predicted $\Delta BC/\Delta CO$. Hereafter, the performance of a predictor in this study refers to a predictor's ability to reproduce observed $\Delta BC/\Delta CO$ via curve-fitting (Sect. 2.5; Fig. 1). A threshold of Pearson $R > 0.71$ ($R^2 > 0.50$) was used to narrow our analysis to predictors that were able to produce predicted $\Delta BC/\Delta CO$ that captured trends in observed $\Delta BC/\Delta CO$. We note that no APT-related predictor met this R threshold, suggesting that APT may not be a good predictor of $\Delta BC/\Delta CO$ and, by extension, aerosol scavenging. One explanation is that APT does not account for different precipitation characteristics such as precipitation frequency or intensity, both of which have been argued to be important for regulating aerosol scavenging (Hou et al., 2018; Wang et al., 2021c). To explore this possibility further, we calculated PA, PF, and PI for each trajectory (Sect. 2.4). Among these three, PF resulted in the most predictors satisfying the minimum R of 0.71. Several PF-related variables in Fig. 2 have R over 0.71, even when accounting for the 25th and 75th percentile error bars derived from k-fold cross-validation. In comparison, only one PA-related predictor ($PA_{48H, IMERG}$; Fig. 2a) and one PI-related predictor ($PI_{PCP > 0.2mm, 48H, P-CDR}$; Fig. 2b) pass the $R > 0.71$ threshold, which indicates that $\Delta BC/\Delta CO$ predicted by PA- or PI-related variables do not track observed $\Delta BC/\Delta CO$ as well as PF-predicted $\Delta BC/\Delta CO$. These results suggest that PF may be more important than PA and PI for predicting aerosol scavenging over the tropical West Pacific.

Noticeably, only one precipitation-related predictor calculated from GFS met the R threshold ($PI_{PCP > 0.2mm, 72H, GFS}$; Fig. 2b). This suggests that GFS-derived precipitation variables are not able to capture observed $\Delta BC/\Delta CO$ trends in contrast to several SPP-based precipitation variables that showed moderate to strong $R (> 0.71)$ with $\Delta BC/\Delta CO$. The poor performance of GFS-derived precipitation is reflective of past studies showing disagreements in precipitation characteristics between satellite and reanalyses (Cannon et al., 2017; Jiang et al., 2021) and even divergent precipitation trends and amounts among individual reanalysis products (Alexander et al., 2020; Chen et al., 2020b; Barrett et al., 2020). Our results suggest that precipitation from GFS reanalysis



is not a reliable predictor of aerosol scavenging compared to precipitation from SPPs. Future studies relating precipitation to aerosol
220 scavenging are recommended to instead rely on in situ or satellite retrieved precipitation rather than precipitation from reanalysis.

Predictors based on quantiles of RH (e.g., RH_{q90}) perform quite well based on R, slope (Fig. 2e), intercept, and WAD (Fig.
2e). RH_{q90} performs slightly better than other RH thresholds (Fig. 2e); however, this difference is minor as shown by the
overlapping 25th-75th percentile error bars between the different RH thresholds. The similar performance between different RH
225 quantiles suggests consistency in their ability to predict $\Delta BC/\Delta CO$ trends (high R) while doing reasonably better than other types
of predictors when estimating $\Delta BC/\Delta CO$ magnitudes across the spectrum of predictor values (intercepts closer to 0, slopes closer
to 1). Maximum RH along trajectories was used by Kanaya et al. (2016) in their analysis of $\Delta BC/\Delta CO$ scavenging to detect the
role of clouds in BC removal. Our findings suggest that top quantiles of RH, including its maximum, are a good choice for
predicting scavenging trends.

Compared to variables directly linked to precipitation (PA, PF, PI, APT), the slopes from RH quantiles are noticeably closer
230 to the ideal value of 1 (Fig. 2e) while intercepts from RH quantiles are closer to the ideal value of 0 (Fig. 2e), meaning $\Delta BC/\Delta CO$
predicted by RH quantiles more closely matches the magnitude of observed $\Delta BC/\Delta CO$ compared to $\Delta BC/\Delta CO$ predicted by
precipitation. We hypothesize that the better performance of RH-related predictors over those more directly related to precipitation
(e.g., APT) may be explained by instances of precipitation that is missed (or misestimated) by SPP retrievals that is indirectly
detected by reanalysis as high humidity conditions. This possibility is supported by previous literature showing the tendency of
235 SPPs to misestimate light (Nadeem et al., 2022; Kidd et al., 2021) or intense precipitation (Chen et al., 2020a; Gupta et al., 2020);
however, our hypothesis of the connection between RH from reanalysis and precipitation from SPPs requires further investigation
in future work.

Of all the fractional predictors considered in this study, f_{MR15} and f_{RH95} perform the best (Fig. 2d). Interestingly, the 25th-75th
percentile range of slopes from f_{RH95} (0.81 – 1.20; Fig. 2d) overlaps with the ideal value of 1 and its intercepts (~ -0.25 ; Fig. 2d) are
240 lower than the other predictors in Fig. 2. These slope and intercept statistics indicate that f_{RH95} is capable estimating the magnitude
of $\Delta BC/\Delta CO$ throughout the spectrum of f_{RH95} values, meaning that f_{RH95} can be used to capture $\Delta BC/\Delta CO$ trends and magnitudes
for both high- $\Delta BC/\Delta CO$ (fresh) and low- $\Delta BC/\Delta CO$ (scavenged) air masses. A similar performance is observed for f_{MR15} . f_{MR15}
and f_{RH95} are similar to PF, which was the best-performing category of precipitation-related predictors, in that PF, f_{MR15} , and f_{RH95}
represent the occurrence frequencies of some condition along each trajectory (e.g., non-zero precipitation or $RH > 95\%$). The better
245 performance of these frequency-related predictors compared to other types of predictors suggests that the frequency of precipitation
or high-RH conditions may be more reliable indicators of aerosol scavenging than the magnitude of precipitation (e.g., APT, PI,
PA).

One limitation of our analysis is the goodness-of-fit achieved during the k-fold cross-validation process as the goodness-of-fit
affects the validity of interpreting the resulting performance statistics (e.g., slope). Fig. S1 of the Supplementary Information (SI)
250 shows no large difference in the goodness-of-fit between different predictors based on R and RMSE. Similar magnitudes of RMSE
(Fig. S1) suggest that the interpretation of performance statistics derived from the curve-fitting procedure is equally valid across
the discussed predictors.

3.2 Nonlinear sensitivity of $\Delta BC/\Delta CO$ to meteorological variables

Although the predictors in Figs. 2 – 3 exhibit the highest R of all predictors considered in this study, their slopes are generally
255 below 1 (Fig. 2) while their intercepts and WAD are generally positive (Fig. 3). The combination of these statistics implies that
predictions of $\Delta BC/\Delta CO$ using our method tend to overestimate observed $\Delta BC/\Delta CO$ across the spectrum of predictor values
(indicated by $WAD > 0$) with maximum overestimations occurring when observed $\Delta BC/\Delta CO$ is low (indicated by slopes < 1 and



intercepts > 0). This points to a nonlinear sensitivity of $\Delta BC/\Delta CO$ to these predictors as the degree of scavenging increases. Dadashazar et al. (2021) observed a similar nonlinear response to APT by a ratio of particulate matter below $2.5 \mu\text{m}$ to CO ($\Delta PM_{2.5}/\Delta CO$), where $\Delta PM_{2.5}/\Delta CO$ was most responsive to APT when APT was below 5 mm and less sensitive to APT when APT exceeded 5 mm.

Investigating this sensitivity further, Fig. 4 shows that PF-predicted $\Delta BC/\Delta CO$ does not capture the trends of observed $\Delta BC/\Delta CO$ for highly scavenged air masses. In other words, PF loses its predictive power as the degree of scavenging increases, implying that PF is most important for the scavenging of fresher air masses (high- $\Delta BC/\Delta CO$). This nonlinear sensitivity of $\Delta BC/\Delta CO$ to PF hints at the possibility that other meteorological variables may become important for further scavenging of highly scavenged air (low- $\Delta BC/\Delta CO$). In contrast to predictors directly related to precipitation (Fig. 4d-f), the predicted curves of RH_{q95} (Fig. 4a), f_{RH95} (Fig. 4b), and f_{MR15} (Fig. 4c) visibly track the trends of observed $\Delta BC/\Delta CO$ with approximately half the difference between predicted and observed $\Delta BC/\Delta CO$ when $\Delta BC/\Delta CO$ is low. The capability of RH_{q95} , f_{RH95} , and f_{MR15} to predict $\Delta BC/\Delta CO$ across a wider range of values is further reflected by generally lower intercepts and WAD (Fig. 3) than precipitation-related predictors, which suggests promising alternative indicators of aerosol scavenging. However, we also note that such differences could arise partly from the limitations of curve-fitting, wherein fitted curves naturally capture gradual changes (e.g., Fig. 4b) better than sharp ones (e.g., Fig. 4d).

3.3 Effect of filtering APT on performance

To improve the predictive performance of precipitation-related variables, we applied combinations of filters for (1) precipitation intensity, (2) trajectory altitude, (3) data product, and (4) trajectory length. Filtering for precipitation intensity isolates the contribution of higher precipitation intensities towards a predictor's ability to predict $\Delta BC/\Delta CO$. Intense precipitation has been shown to be more efficient at scavenging aerosol particles (Zhao et al., 2020) and may be important when estimating aerosol scavenging. Filtering for trajectory altitude (i.e., considering precipitation only when the trajectory altitude is below 1.5 km AGL) tests the hypothesis that air masses within the boundary layer will be most susceptible to wet scavenging. Grythe et al. (2017) demonstrated that below-cloud scavenging (i.e., impaction by precipitation) accounted for majority of scavenging events below 1 km. We selected 1.5 km based on previous work on the marine boundary layer over the tropical West Pacific (Chien et al., 2019). We repeated the analysis for three precipitation products (one reanalysis and two SPPs) to capture variability in our results due to the choice of data product which has been shown to be important for precipitation (Alexander et al., 2020). Finally, we tested the effect of trajectory length on the performance of APT as a predictor of $\Delta BC/\Delta CO$.

In general, we found that applying altitude and/or precipitation filters negatively affected the performance of APT (Fig. 5b-d), leading to lower R between predicted and observed $\Delta BC/\Delta CO$ compared to the case without any filters applied (Fig. 5a). The poorer performance of precipitation filtered for higher intensities (Fig. 5b) suggests that these higher intensities may not be as important for estimating wet scavenging compared to low intensity precipitation, consistent with previous work showing that light rain exerts more control over the global aerosol burden (Wang et al., 2021b) and that precipitation over the tropical West Pacific is typically high in frequency and low to moderate in intensity (Biasutti et al., 2012).

Applying a filter for trajectory altitude prior to calculating APT also did not lead to improvements in R (Fig. 5c). This was surprising because, when using total column precipitation from SPPs, a maximum altitude filter should reduce errors from cases where precipitation occurs below the air mass and no scavenging occurs. Since the SPPs used in this study have been validated using surface measurements (Sapiano and Arkin, 2009; Nicholson et al., 2019; Wang et al., 2021a), precipitation from SPPs should be reflective of precipitation that reaches the surface, implying a susceptibility of these SPPs to errors related to virga (Wang et al., 2018). However, Wang et al. (2018) also showed that virga occurrence over the tropical West Pacific is also infrequent. An



alternative explanation for the poor performance of altitude-filtered predictors is uncertainties related to trajectory altitude (Harris et al., 2005), such that an air parcel may have actually been traveling at a lower altitude than its modelled trajectory and underwent scavenging.

300 An examination of trajectory altitudes (Fig. S5) revealed that filtering for trajectory altitudes below 1.5 km excluded the majority (~70%) of precipitating grid cells encountered by trajectories, which likely negatively impacted the predictive ability of altitude-filtered predictors.

305 Longer trajectories resulted in slightly higher R between observed and APT-predicted $\Delta BC/\Delta CO$ (Fig. 5a-b), increasing from R ~0.5 to ~0.6; however, this difference is not large, as shown by overlapping 25th-75th percentile error bars. Interestingly, this increase in R for longer trajectories was more evident when filtering for precipitation intensities $> 0.2 \text{ mm h}^{-1}$ when calculating APT (Fig. 5b) or PI (Fig. S2b), but not when applying this intensity filter on PF (Fig. S3b) or PA (Fig. S4b). Further interpretation likely requires a physical model in future work to explain why the performance of intense precipitation (Fig. 5b) benefits from a longer trajectory more than total precipitation does (Fig. 5a).

4 Limitations

310 **$\Delta BC/\Delta CO$ as a wet scavenging proxy:** In this study, we treat $\Delta BC/\Delta CO$ as a proxy for wet scavenging (i.e., predictand) and base our conclusions on which variables best predict this ratio (i.e., predictors). An underlying assumption is that there is negligible emission of BC or CO after initial emission and after wet scavenging occurs. Consequently, this method is expected to work well in outflow regions such as the tropical West Pacific and not well where additional BC and/or CO are likely to be after initial emission or wet scavenging has occurred (e.g., continental region).

315 **$\Delta BC/\Delta CO$ depends on air mass type:** The $\Delta BC/\Delta CO$ quantity is also affected by air mass type. For example, biomass burning and anthropogenic/industrial emissions will have different $\Delta BC/\Delta CO$ values (e.g., Hilario et al., 2021). The mixing state and composition of BC-containing particles will also affect its hygroscopicity and by extension its rate of wet scavenging (Liu et al., 2013). Although these factors are expected to influence $\Delta BC/\Delta CO$, we assume the response of $\Delta BC/\Delta CO$ to the predictor will be chiefly determined by scavenging-related processes. While the response of $\Delta BC/\Delta CO$ to APT in Hilario et al. (2021) was quite similar across different air mass origins (their Fig. 9), this may not be always the case. However, this origin-independent relationship does allow for the option of curve-fitting without differentiating between individual sources. Beneficially, this choice to aggregate the data rather than resolving by source increases the number of data points available for curve-fitting, which improves the robustness of the resulting statistics and adds strength to our conclusions on which meteorological variables are most relevant for aerosol scavenging.

325 **Specific processes:** The conclusions of our study are based on the relative ability of different variables to predict $\Delta BC/\Delta CO$, our proxy for wet scavenging. This approach does not isolate individual processes that are usually parameterized by global circulation models (e.g., impaction, nucleation) (Croft et al., 2009, 2010; Ryu and Min, 2022). However, through our proposed framework, we can still gain qualitative insights into which meteorological variables are relevant for estimating aerosol scavenging, which can inform future studies as well as developments in model parametrization.

330 **Single predictor method:** The method presented here assesses the one-to-one relationship between a single predictor and $\Delta BC/\Delta CO$ repeated individually for several predictors. We expect that using a combination of predictors may lead to better predictions of $\Delta BC/\Delta CO$ while providing a more physical picture of relative contributions of different meteorological variables towards wet scavenging. Future work may utilize multiple linear regression or more sophisticated methods such as machine learning to consider different combinations of predictors with the objective of identifying a combination that predicts $\Delta BC/\Delta CO$



335 well and extracting further information on what physical mechanisms may be relevant for the removal of $\Delta BC/\Delta CO$ based on relative coefficients or weightings of different predictors.

Curve-fitting: The results can depend on the curve-fitting function used. Different variables are expected to have different relationships with $\Delta BC/\Delta CO$. Thus, if we considered only one function for curve-fitting, it would favor variables that have a specific relationship with $\Delta BC/\Delta CO$. To reduce this bias, we applied four different curve-fitting functions on each predictor based on previous studies (Table 2) that accounted for possible relationships between $\Delta BC/\Delta CO$ and each predictor. We then chose the
340 curve-fitting function that produced the highest R between observed and predicted $\Delta BC/\Delta CO$. However, we note that this does not completely remove the bias as specific functions were still selected.

Trajectory modeling: Vertical motion through convection, entrainment, and detrainment processes are known uncertainties in trajectory modeling, which increase with trajectory length (Harris et al., 2005). The spatial and temporal resolutions of the meteorological input used for the HYSPLIT model are also limiting factors as meteorology along HYSPLIT trajectories do not
345 account for sub-timestep or sub-grid processes.

5 Conclusions

We present a method to identify meteorological indicators of aerosol scavenging using a combination of aircraft, satellite, and reanalysis data coupled with HYSPLIT backward trajectories. We apply this method to the CAMP²Ex field campaign over the
350 tropical West Pacific, which hosts a wide range of cloud fractions and precipitation characteristics as well as an environment characterized by long-range transport of aerosol and trace gas species. Since $\Delta BC/\Delta CO$ is mainly affected by scavenging, we treat $\Delta BC/\Delta CO$ as an in situ proxy for aerosol scavenging and evaluate the responses of $\Delta BC/\Delta CO$ to different meteorological variables (i.e., predictors). The main conclusions of the study are the following:

1. Although APT has been utilized in several studies as an indicator of aerosol scavenging, we demonstrated that APT-
355 predicted $\Delta BC/\Delta CO$ does not track observed $\Delta BC/\Delta CO$ well. Furthermore, the application of altitude or precipitation intensity filters negatively impacted the performance of APT in predicting $\Delta BC/\Delta CO$ trends. Since APT is an accumulated precipitation amount over the whole trajectory, APT does not account for other precipitation characteristics such as intensity or frequency, which have been shown to be relevant for aerosol scavenging. This shortcoming may explain the overall poor relative performance of APT in predicting $\Delta BC/\Delta CO$.
- 360 2. To investigate which precipitation characteristics are most relevant for predicting aerosol scavenging, we calculated PA, PF, and PI along trajectories using precipitation from reanalysis (GFS) and SPPs (IMERG, PERSIANN-CDR). While several precipitation-related predictors calculated from SPPs were able to predict $\Delta BC/\Delta CO$ reasonably well, only one precipitation-related predictor from GFS correlated with $\Delta BC/\Delta CO$ ($R > 0.71$), suggesting that precipitation from SPPs may be better at predicting aerosol scavenging than precipitation from reanalysis. The poorer performance of precipitation
365 from reanalysis in predicting $\Delta BC/\Delta CO$ than from SPPs is corroborated by previous studies that found larger misestimates of precipitation by reanalysis than by SPPs. Because of our results and those of past studies, we recommend relying on in situ or SPP precipitation rather than precipitation from reanalysis, particularly when relating precipitation to aerosol scavenging.
- 370 3. Frequency-related predictors such as PF, f_{MR15} , and f_{RH95} performed much better than APT in predicting $\Delta BC/\Delta CO$ trends and magnitudes. PF, f_{MR15} , and f_{RH95} represent the frequencies of occurrence of some meteorological condition along trajectories such as non-zero precipitation (PF) or RH exceeding 95% (f_{RH95}). The relatively better performance of these



frequency-related predictors over those related to PA or PI suggests that the frequency of precipitation or high-RH conditions may be a more reliable indicator of aerosol scavenging than the magnitude of precipitation.

375 4. Predictors based on specific quantiles or the mean of RH also performed quite well in predicting both $\Delta BC/\Delta CO$ trends and magnitudes. We found only minor differences in the performance depending on the exact quantile used. We hypothesize the outperformance of RH quantiles over predictors more directly related to precipitation (e.g., APT) to be due to missed precipitation in SPP retrievals that was indirectly represented in reanalysis as high humidity conditions. Such a possibility is supported by previous literature demonstrating that SPPs tend to misestimate light precipitation (Nadeem et al., 2022; Kidd et al., 2021); however, further work is required to explore this hypothesis.

380 By identifying which meteorological variables are relevant for predicting $\Delta BC/\Delta CO$ trends (and by extension, aerosol wet scavenging), the findings of this study may be useful for informing future aerosol scavenging studies. Furthermore, these results may also aid in improving scavenging parametrization schemes in models. The method presented in this study is repeatable over a variety of environments and is relatively computationally inexpensive to apply. Future work may utilize machine learning to identify combinations of meteorological variables to predict aerosol scavenging and apply our method to different regions to identify region-specific indicators of aerosol scavenging. Furthermore, CAMP²Ex included a rich dataset on cloud water composition (Crosbie et al., 2022; Stahl et al., 2021) that can be explored, as in past work for other regions (MacDonald et al., 2018), to gain additional insights into aerosol wet scavenging processes.

Code availability. Codes are freely available upon request to the authors.

390 *Data availability.* All datasets are publicly available and accessible at <https://doi.org/10.5067/Suborbital/CAMP2EX2018/DATA001> (NASA/LaRC/SD/ASDC, 2020). HYSPLIT data are accessible through the NOAA READY website (<https://www.ready.noaa.gov/index.php>, last access: 11 April 2023) (NOAA Physical Sciences Laboratory, 2020).

Author contributions. EC, LDZ, MAS, JPD, GSD contributed to data collection. MRAH and AS conceptualized the study. MRAH performed the data analysis and prepared the manuscript with input from all co-authors.

Competing interests. The authors declare that they have no conflict of interest.

Disclaimer. Publisher's note: Copernicus Publications remains neutral with regard to jurisdictional claims in published maps and institutional affiliations.

400 *Special issue statement.* This article is part of the special issue "Cloud Aerosol and Monsoon Processes Philippines Experiment (CAMP²Ex) (ACP/AMT inter-journal SI)". It is not associated with a conference.

Acknowledgements. This research has been supported by the National Aeronautics and Space Administration (grant no. 80NSSC18K0148).



6 References

405 Alexander, L. V., Bador, M., Roca, R., Contractor, S., Donat, M. G., and Nguyen, P. L.: Intercomparison of annual precipitation indices and extremes over global land areas from in situ, space-based and reanalysis products, *Environ. Res. Lett.*, 15, 055002, <https://doi.org/10.1088/1748-9326/ab79e2>, 2020.

Andronache, C.: Estimated variability of below-cloud aerosol removal by rainfall for observed aerosol size distributions, *Atmospheric Chemistry and Physics*, 3, 131–143, <https://doi.org/10.5194/acp-3-131-2003>, 2003.

410 NOAA Physical Sciences Laboratory: <https://psl.noaa.gov/data/gridded/index.html>, last access: 13 June 2020.

Ashouri, H., Hsu, K.-L., Sorooshian, S., Braithwaite, D. K., Knapp, K. R., Cecil, L. D., Nelson, B. R., and Prat, O. P.: PERSIANN-CDR: Daily Precipitation Climate Data Record from Multisatellite Observations for Hydrological and Climate Studies, *Bull. Amer. Meteor. Soc.*, 96, 69–83, <https://doi.org/10.1175/BAMS-D-13-00068.1>, 2015.

Barrett, A. P., Stroeve, J. C., and Serreze, M. C.: Arctic Ocean Precipitation From Atmospheric Reanalyses and Comparisons With North Pole Drifting Station Records, *Journal of Geophysical Research: Oceans*, 125, e2019JC015415, <https://doi.org/10.1029/2019JC015415>, 2020.

Bellouin, N., Quaas, J., Gryspeerdt, E., Kinne, S., Stier, P., Watson-Parris, D., Boucher, O., Carslaw, K. S., Christensen, M., Daniau, A.-L., Dufresne, J.-L., Feingold, G., Fiedler, S., Forster, P., Gettelman, A., Haywood, J. M., Lohmann, U., Malavelle, F., Mauritsen, T., McCoy, D. T., Myhre, G., Mülmenstädt, J., Neubauer, D., Possner, A., Rugenstein, M., Sato, Y., Schulz, M., Schwartz, S. E., Sourdeval, O., Storelvmo, T., Toll, V., Winker, D., and Stevens, B.: Bounding Global Aerosol Radiative Forcing of Climate Change, *Reviews of Geophysics*, 58, e2019RG000660, <https://doi.org/10.1029/2019RG000660>, 2020.

Biasutti, M., Yuter, S. E., Burleyson, C. D., and Sobel, A. H.: Very high resolution rainfall patterns measured by TRMM precipitation radar: seasonal and diurnal cycles, *Clim Dyn*, 39, 239–258, <https://doi.org/10.1007/s00382-011-1146-6>, 2012.

Cannon, F., Ralph, F. M., Wilson, A. M., and Lettenmaier, D. P.: GPM Satellite Radar Measurements of Precipitation and Freezing Level in Atmospheric Rivers: Comparison With Ground-Based Radars and Reanalyses, *Journal of Geophysical Research: Atmospheres*, 122, 12,747–12,764, <https://doi.org/10.1002/2017JD027355>, 2017.

Chen, H., Yong, B., Qi, W., Wu, H., Ren, L., and Hong, Y.: Investigating the Evaluation Uncertainty for Satellite Precipitation Estimates Based on Two Different Ground Precipitation Observation Products, *Journal of Hydrometeorology*, 21, 2595–2606, <https://doi.org/10.1175/JHM-D-20-0103.1>, 2020a.

430 Chen, S., Liu, B., Tan, X., and Wu, Y.: Inter-comparison of spatiotemporal features of precipitation extremes within six daily precipitation products, *Clim Dyn*, 54, 1057–1076, <https://doi.org/10.1007/s00382-019-05045-z>, 2020b.

Chien, F.-C., Hong, J.-S., and Kuo, Y.-H.: The Marine Boundary Layer Height over the Western North Pacific Based on GPS Radio Occultation, Island Soundings, and Numerical Models, *Sensors*, 19, 155, <https://doi.org/10.3390/s19010155>, 2019.

435 Choi, Y., Kanaya, Y., Takigawa, M., Zhu, C., Park, S.-M., Matsuki, A., Sadanaga, Y., Kim, S.-W., Pan, X., and Pisso, I.: Investigation of the wet removal rate of black carbon in East Asia: validation of a below- and in-cloud wet removal scheme in



FLEXible PARTicle (FLEXPART) model v10.4, *Atmospheric Chemistry and Physics*, 20, 13655–13670, <https://doi.org/10.5194/acp-20-13655-2020>, 2020.

Coelho, L. P.: Jug: Software for Parallel Reproducible Computation in Python, 5, 30, <https://doi.org/10.5334/jors.161>, 2017.

440 Croft, B., Lohmann, U., Martin, R. V., Stier, P., Wurzler, S., Feichter, J., Posselt, R., and Ferrachat, S.: Aerosol size-dependent below-cloud scavenging by rain and snow in the ECHAM5-HAM, *Atmos. Chem. Phys.*, 23, 2009.

Croft, B., Lohmann, U., Martin, R. V., Stier, P., Wurzler, S., Feichter, J., Hoose, C., Heikkilä, U., van Donkelaar, A., and Ferrachat, S.: Influences of in-cloud aerosol scavenging parameterizations on aerosol concentrations and wet deposition in ECHAM5-HAM, *Atmos. Chem. Phys.*, 33, 2010.

445 Crosbie, E., Ziemba, L. D., Shook, M. A., Robinson, C. E., Winstead, E. L., Thornhill, K. L., Braun, R. A., MacDonald, A. B., Stahl, C., Sorooshian, A., van den Heever, S. C., DiGangi, J. P., Diskin, G. S., Woods, S., Bañaga, P., Brown, M. D., Gallo, F., Hilario, M. R. A., Jordan, C. E., Leung, G. R., Moore, R. H., Sanchez, K. J., Shingler, T. J., and Wiggins, E. B.: Measurement report: Closure analysis of aerosol–cloud composition in tropical maritime warm convection, *Atmospheric Chemistry and Physics*, 22, 13269–13302, <https://doi.org/10.5194/acp-22-13269-2022>, 2022.

450 Dadashazar, H., Alipanah, M., Hilario, M. R. A., Crosbie, E., Kirschler, S., Liu, H., Moore, R. H., Peters, A. J., Scarino, A. J., Shook, M., Thornhill, K. L., Voigt, C., Wang, H., Winstead, E., Zhang, B., Ziemba, L., and Sorooshian, A.: Aerosol responses to precipitation along North American air trajectories arriving at Bermuda, *Atmospheric Chemistry and Physics*, 21, 16121–16141, <https://doi.org/10.5194/acp-21-16121-2021>, 2021.

Feng, J.: A 3-mode parameterization of below-cloud scavenging of aerosols for use in atmospheric dispersion models, *Atmospheric Environment*, 41, 6808–6822, <https://doi.org/10.1016/j.atmosenv.2007.04.046>, 2007.

455 Flossmann, A. I., Hall, W. D., and Pruppacher, H. R.: A Theoretical Study of the Wet Removal of Atmospheric Pollutants. Part I: The Redistribution of Aerosol Particles Captured through Nucleation and Impaction Scavenging by Growing Cloud Drops, *Journal of the Atmospheric Sciences*, 42, 583–606, [https://doi.org/10.1175/1520-0469\(1985\)042<0583:ATSOTW>2.0.CO;2](https://doi.org/10.1175/1520-0469(1985)042<0583:ATSOTW>2.0.CO;2), 1985.

460 Frey, L., Bender, F. A.-M., and Svensson, G.: Processes controlling the vertical aerosol distribution in marine stratocumulus regions – a sensitivity study using the climate model NorESM1-M, *Atmospheric Chemistry and Physics*, 21, 577–595, <https://doi.org/10.5194/acp-21-577-2021>, 2021.

Grythe, H., Kristiansen, N. I., Groot Zwaafink, C. D., Eckhardt, S., Ström, J., Tunved, P., Krejci, R., and Stohl, A.: A new aerosol wet removal scheme for the Lagrangian particle model FLEXPART v10, *Geoscientific Model Development*, 10, 1447–1466, <https://doi.org/10.5194/gmd-10-1447-2017>, 2017.

465 Gupta, V., Jain, M. K., Singh, P. K., and Singh, V.: An assessment of global satellite-based precipitation datasets in capturing precipitation extremes: A comparison with observed precipitation dataset in India, *International Journal of Climatology*, 40, 3667–3688, <https://doi.org/10.1002/joc.6419>, 2020.



Harris, J. M., Draxler, R. R., and Oltmans, S. J.: Trajectory model sensitivity to differences in input data and vertical transport method, *J. Geophys. Res.-Atmos.*, 110, D14109, <https://doi.org/10.1029/2004JD005750>, 2005.

470 Hilario, M. R. A., Olaguera, L. M., Narisma, G. T., and Matsumoto, J.: Diurnal Characteristics of Summer Precipitation Over Luzon Island, Philippines, *Asia-Pacific J Atmos Sci*, <https://doi.org/10.1007/s13143-020-00214-1>, 2020.

Hilario, M. R. A., Crosbie, E., Shook, M., Reid, J. S., Cambaliza, M. O. L., Simpas, J. B. B., Ziemba, L., DiGangi, J. P., Diskin, G. S., Nguyen, P., Turk, F. J., Winstead, E., Robinson, C. E., Wang, J., Zhang, J., Wang, Y., Yoon, S., Flynn, J., Alvarez, S. L., Behrangi, A., and Sorooshian, A.: Measurement report: Long-range transport patterns into the tropical northwest Pacific during the CAMP²Ex aircraft campaign: chemical composition, size distributions, and the impact of convection, *Atmospheric Chemistry and Physics*, 21, 3777–3802, <https://doi.org/10.5194/acp-21-3777-2021>, 2021.

Hilario, M. R. A., Bañaga, P. A., Betito, G., Braun, R. A., Cambaliza, M. O., Cruz, M. T., Lorenzo, G. R., MacDonald, A. B., Pabroa, P. C., Simpas, J. B., Stahl, C., Yee, J. R., and Sorooshian, A.: Stubborn aerosol: why particulate mass concentrations do not drop during the wet season in Metro Manila, Philippines, *Environ. Sci.: Atmos.*, 2, 1428–1437, <https://doi.org/10.1039/D2EA00073C>, 2022.

Hodzic, A., Kasibhatla, P. S., Jo, D. S., Cappa, C. D., Jimenez, J. L., Madronich, S., and Park, R. J.: Rethinking the global secondary organic aerosol (SOA) budget: stronger production, faster removal, shorter lifetime, *Atmospheric Chemistry and Physics*, 16, 7917–7941, <https://doi.org/10.5194/acp-16-7917-2016>, 2016.

Hou, P., Wu, S., McCarty, J. L., and Gao, Y.: Sensitivity of atmospheric aerosol scavenging to precipitation intensity and frequency in the context of global climate change, *Atmospheric Chemistry and Physics*, 18, 8173–8182, <https://doi.org/10.5194/acp-18-8173-2018>, 2018.

Huffman, G. J., Bolvin, D. T., Braithwaite, D., Hsu, K.-L., Joyce, R. J., Kidd, C., Nelkin, E. J., Sorooshian, S., Stocker, E. F., Tan, J., Wolff, D. B., and Xie, P.: Integrated Multi-satellite Retrievals for the Global Precipitation Measurement (GPM) Mission (IMERG), in: *Satellite Precipitation Measurement: Volume 1*, edited by: Levizzani, V., Kidd, C., Kirschbaum, D. B., Kummerow, C. D., Nakamura, K., and Turk, F. J., Springer International Publishing, Cham, 343–353, https://doi.org/10.1007/978-3-030-24568-9_19, 2020.

Jensen, J. B. and Charlson, R. J.: On the efficiency of nucleation scavenging, *Tellus B*, 36B, 367–375, <https://doi.org/10.1111/j.1600-0889.1984.tb00255.x>, 1984.

Jiang, Q., Li, W., Fan, Z., He, X., Sun, W., Chen, S., Wen, J., Gao, J., and Wang, J.: Evaluation of the ERA5 reanalysis precipitation dataset over Chinese Mainland, *Journal of Hydrology*, 595, 125660, <https://doi.org/10.1016/j.jhydrol.2020.125660>, 2021.

Kanaya, Y., Pan, X., Miyakawa, T., Komazaki, Y., Taketani, F., Uno, I., and Kondo, Y.: Long-term observations of black carbon mass concentrations at Fukue Island, western Japan, during 2009–2015: constraining wet removal rates and emission strengths from East Asia, *Atmospheric Chemistry and Physics*, 16, 10689–10705, <https://doi.org/10.5194/acp-16-10689-2016>, 2016.



Kanaya, Y., Yamaji, K., Miyakawa, T., Taketani, F., Zhu, C., Choi, Y., Komazaki, Y., Ikeda, K., Kondo, Y., and Klimont, Z.: Rapid reduction in black carbon emissions from China: evidence from 2009–2019 observations on Fukue Island, Japan, *Atmospheric Chemistry and Physics*, 20, 6339–6356, <https://doi.org/10.5194/acp-20-6339-2020>, 2020.

505 Kidd, C., Graham, E., Smyth, T., and Gill, M.: Assessing the Impact of Light/Shallow Precipitation Retrievals from Satellite-Based Observations Using Surface Radar and Micro Rain Radar Observations, *Remote Sensing*, 13, 1708, <https://doi.org/10.3390/rs13091708>, 2021.

Kim, K. D., Lee, S., Kim, J.-J., Lee, S.-H., Lee, D., Lee, J.-B., Choi, J.-Y., and Kim, M. J.: Effect of Wet Deposition on Secondary Inorganic Aerosols Using an Urban-Scale Air Quality Model, *Atmosphere*, 12, 168, <https://doi.org/10.3390/atmos12020168>, 2021.

510 Kipling, Z., Stier, P., Johnson, C. E., Mann, G. W., Bellouin, N., Bauer, S. E., Bergman, T., Chin, M., Diehl, T., Ghan, S. J., Iversen, T., Kirkevåg, A., Kokkola, H., Liu, X., Luo, G., van Noije, T., Pringle, K. J., von Salzen, K., Schulz, M., Seland, Ø., Skeie, R. B., Takemura, T., Tsigaridis, K., and Zhang, K.: What controls the vertical distribution of aerosol? Relationships between process sensitivity in HadGEM3–UKCA and inter-model variation from AeroCom Phase II, *Atmos. Chem. Phys.*, 16, 2221–2241, <https://doi.org/10.5194/acp-16-2221-2016>, 2016.

515 Kleinman, L. I., Daum, P. H., Lee, Y.-N., Senum, G. I., Springston, S. R., Wang, J., Berkowitz, C., Hubbe, J., Zaveri, R. A., Brechtel, F. J., Jayne, J., Onasch, T. B., and Worsnop, D.: Aircraft observations of aerosol composition and ageing in New England and Mid-Atlantic States during the summer 2002 New England Air Quality Study field campaign, *J. Geophys. Res.*, 112, D09310, <https://doi.org/10.1029/2006JD007786>, 2007.

520 Koike, M., Kondo, Y., Kita, K., Takegawa, N., Masui, Y., Miyazaki, Y., Ko, M. W., Weinheimer, A. J., Flocke, F., Weber, R. J., Thornton, D. C., Sachse, G. W., Vay, S. A., Blake, D. R., Streets, D. G., Eisele, F. L., Sandholm, S. T., Singh, H. B., and Talbot, R. W.: Export of anthropogenic reactive nitrogen and sulfur compounds from the East Asia region in spring, *J. Geophys. Res.*, 108, 8789, <https://doi.org/10.1029/2002JD003284>, 2003.

525 Kondo, Y., Matsui, H., Moteki, N., Sahu, L., Takegawa, N., Kajino, M., Zhao, Y., Cubison, M. J., Jimenez, J. L., Vay, S., Diskin, G. S., Anderson, B., Wisthaler, A., Mikoviny, T., Fuelberg, H. E., Blake, D. R., Huey, G., Weinheimer, A. J., Knapp, D. J., and Brune, W. H.: Emissions of black carbon, organic, and inorganic aerosols from biomass burning in North America and Asia in 2008, *J. Geophys. Res.*, 116, D08204, <https://doi.org/10.1029/2010JD015152>, 2011.

Lin, C., Huo, T., Yang, F., Wang, B., Chen, Y., and Wang, H.: Characteristics of Water-soluble Inorganic Ions in Aerosol and Precipitation and their Scavenging Ratios in an Urban Environment in Southwest China, *Aerosol Air Qual. Res.*, 21, 200513, <https://doi.org/10.4209/aaqr.200513>, 2021.

530 Liu, D., Allan, J., Whitehead, J., Young, D., Flynn, M., Coe, H., McFiggans, G., Fleming, Z. L., and Bandy, B.: Ambient black carbon particle hygroscopic properties controlled by mixing state and composition, *Atmospheric Chemistry and Physics*, 13, 2015–2029, <https://doi.org/10.5194/acp-13-2015-2013>, 2013.



Liu, M. and Matsui, H.: Improved Simulations of Global Black Carbon Distributions by Modifying Wet Scavenging Processes in Convective and Mixed-Phase Clouds, *Journal of Geophysical Research: Atmospheres*, 126, e2020JD033890, 535 <https://doi.org/10.1029/2020JD033890>, 2021.

Livingston, J. M., Schmid, B., Russell, P. B., Podolske, J. R., Redemann, J., and Diskin, G. S.: Comparison of Water Vapor Measurements by Airborne Sun Photometer and Diode Laser Hygrometer on the NASA DC-8, *Journal of Atmospheric and Oceanic Technology*, 25, 1733–1743, <https://doi.org/10.1175/2008JTECHA1047.1>, 2008.

Lu, X. C. and Fung, J. C. H.: Sensitivity assessment of PM_{2.5} simulation to the below-cloud washout schemes in an atmospheric chemical transport model, *Tellus B: Chemical and Physical Meteorology*, 70, 1–17, 540 <https://doi.org/10.1080/16000889.2018.1476435>, 2018.

Luo, G., Yu, F., and Schwab, J.: Revised treatment of wet scavenging processes dramatically improves GEOS-Chem 12.0.0 simulations of surface nitric acid, nitrate, and ammonium over the United States, *Geoscientific Model Development*, 12, 3439–3447, <https://doi.org/10.5194/gmd-12-3439-2019>, 2019.

MacDonald, A. B., Dadashazar, H., Chuang, P. Y., Crosbie, E., Wang, H., Wang, Z., Jonsson, H. H., Flagan, R. C., Seinfeld, J. H., and Sorooshian, A.: Characteristic Vertical Profiles of Cloud Water Composition in Marine Stratocumulus Clouds and Relationships With Precipitation, *J. Geophys. Res. Atmos.*, 123, 3704–3723, <https://doi.org/10.1002/2017JD027900>, 2018.

Mahmood, R., von Salzen, K., Flanner, M., Sand, M., Langner, J., Wang, H., and Huang, L.: Seasonality of global and Arctic black carbon processes in the Arctic Monitoring and Assessment Programme models, *Journal of Geophysical Research: Atmospheres*, 121, 7100–7116, <https://doi.org/10.1002/2016JD024849>, 2016.

Marinescu, P. J., Heever, S. C. van den, Saleeby, S. M., Kreidenweis, S. M., and DeMott, P. J.: The Microphysical Roles of Lower-Tropospheric versus Midtropospheric Aerosol Particles in Mature-Stage MCS Precipitation, *Journal of the Atmospheric Sciences*, 74, 3657–3678, <https://doi.org/10.1175/JAS-D-16-0361.1>, 2017.

Matsui, H., Kondo, Y., Moteki, N., Takegawa, N., Sahu, L. K., Zhao, Y., Fuelberg, H. E., Sessions, W. R., Diskin, G., Blake, D. R., Wisthaler, A., and Koike, M.: Seasonal variation of the transport of black carbon aerosol from the Asian continent to the Arctic during the ARCTAS aircraft campaign, *J. Geophys. Res.*, 116, D05202, <https://doi.org/10.1029/2010JD015067>, 2011.

Mitra, S. K., Brinkmann, J., and Pruppacher, H. R.: A wind tunnel study on the drop-to-particle conversion, *Journal of Aerosol Science*, 23, 245–256, [https://doi.org/10.1016/0021-8502\(92\)90326-Q](https://doi.org/10.1016/0021-8502(92)90326-Q), 1992.

Moteki, N. and Kondo, Y.: Effects of Mixing State on Black Carbon Measurements by Laser-Induced Incandescence, *Aerosol Science and Technology*, 41, 398–417, <https://doi.org/10.1080/02786820701199728>, 2007.

Moteki, N. and Kondo, Y.: Dependence of Laser-Induced Incandescence on Physical Properties of Black Carbon Aerosols: Measurements and Theoretical Interpretation, *Aerosol Science and Technology*, 44, 663–675, <https://doi.org/10.1080/02786826.2010.484450>, 2010.



565 Moteki, N., Kondo, Y., Oshima, N., Takegawa, N., Koike, M., Kita, K., Matsui, H., and Kajino, M.: Size dependence of wet removal of black carbon aerosols during transport from the boundary layer to the free troposphere, *Geophys. Res. Lett.*, 39, L13802, <https://doi.org/10.1029/2012GL052034>, 2012.

Moteki, N., Mori, T., Matsui, H., and Ohata, S.: Observational constraint of in-cloud supersaturation for simulations of aerosol rainout in atmospheric models, *npj Clim Atmos Sci*, 2, 1–11, <https://doi.org/10.1038/s41612-019-0063-y>, 2019.

570 Murphy, D. M., Cziczo, D. J., Hudson, P. K., Thomson, D. S., Wilson, J. C., Kojima, T., and Buseck, P. R.: Particle Generation and Resuspension in Aircraft Inlets when Flying in Clouds, *Aerosol Science and Technology*, 38, 401–409, <https://doi.org/10.1080/02786820490443094>, 2004.

Nadeem, M. U., Anjum, M. N., Afzal, A., Azam, M., Hussain, F., Usman, M., Javaid, M. M., Mukhtar, M. A., and Majeed, F.: Assessment of Multi-Satellite Precipitation Products over the Himalayan Mountains of Pakistan, South Asia, *Sustainability*, 14, 8490, <https://doi.org/10.3390/su14148490>, 2022.

575 Nguyen, P., Ombadi, M., Sorooshian, S., Hsu, K., AghaKouchak, A., Braithwaite, D., Ashouri, H., and Thorstensen, A. R.: The PERSIANN family of global satellite precipitation data: a review and evaluation of products, *Hydrol. Earth Syst. Sci.*, 22, 5801–5816, <https://doi.org/10.5194/hess-22-5801-2018>, 2018.

Nicholson, S. E., Klotter, D., Zhou, L., and Hua, W.: Validation of Satellite Precipitation Estimates over the Congo Basin, *J. Hydrometeor.*, 20, 631–656, <https://doi.org/10.1175/JHM-D-18-0118.1>, 2019.

580 Oshima, N., Kondo, Y., Moteki, N., Takegawa, N., Koike, M., Kita, K., Matsui, H., Kajino, M., Nakamura, H., Jung, J. S., and Kim, Y. J.: Wet removal of black carbon in Asian outflow: Aerosol Radiative Forcing in East Asia (A-FORCE) aircraft campaign, *J. Geophys. Res.*, 117, n/a-n/a, <https://doi.org/10.1029/2011JD016552>, 2012.

Radke, L. F., Hobbs, P. V., and Eltgroth, M. W.: Scavenging of Aerosol Particles by Precipitation, *Journal of Applied Meteorology and Climatology*, 19, 715–722, [https://doi.org/10.1175/1520-0450\(1980\)019<0715:SOAPBP>2.0.CO;2](https://doi.org/10.1175/1520-0450(1980)019<0715:SOAPBP>2.0.CO;2), 1980.

585 Reid, J. S., Maring, H. B., Narisma, G. T., Heever, S. van den, Girolamo, L. D., Ferrare, R., Lawson, P., Mace, G. G., Simpas, J. B., Tanelli, S., Ziemba, L., Diederhoven, B. van, Brientjes, R., Bucholtz, A., Cairns, B., Cambaliza, M. O., Chen, G., Diskin, G. S., Flynn, J. H., Hostetler, C. A., Holz, R. E., Lang, T. J., Schmidt, K. S., Smith, G., Sorooshian, A., Thompson, E. J., Thornhill, K. L., Trepte, C., Wang, J., Woods, S., Yoon, S., Alexandrov, M., Alvarez, S., Amiot, C. G., Bennett, J. R., M., B., Burton, S. P., Cayan, E., Chen, H., Collow, A., Crosbie, E., DaSilva, A., DiGangi, J. P., Flagg, D. D., Freeman, S. W., Fu, D., Fukada, E.,
590 Hilario, M. R. A., Hong, Y., Hristova-Velva, S. M., Kuehn, R., Kowch, R. S., Leung, G. R., Loveridge, J., Meyer, K., Miller, R. M., Montes, M. J., Moum, J. N., Nenes, T., Nesbitt, S. W., Norgren, M., Nowotnick, E. P., Rauber, R. M., Reid, E. A., Rutledge, S., Schlosser, J. S., Sekiyama, T. T., Shook, M. A., Sokolowsky, G. A., Stamnes, S. A., Tanaka, T. Y., Wasilewski, A., Xian, P., Xiao, Q., Xu, Z., and Zavaleta, J.: The coupling between tropical meteorology, aerosol lifecycle, convection, and radiation, during the Cloud, Aerosol and Monsoon Processes Philippines Experiment (CAMP2Ex), *Bulletin of the American Meteorological Society*, 1, <https://doi.org/10.1175/BAMS-D-21-0285.1>, 2023.



Rolph, G., Stein, A., and Stunder, B.: Real-time Environmental Applications and Display sYstem: READY, *Environmental Modelling & Software*, 95, 210–228, <https://doi.org/10.1016/j.envsoft.2017.06.025>, 2017.

Ryu, Y.-H. and Min, S.-K.: Improving Wet and Dry Deposition of Aerosols in WRF-Chem: Updates to Below-Cloud Scavenging and Coarse-Particle Dry Deposition, *Journal of Advances in Modeling Earth Systems*, 14, e2021MS002792, <https://doi.org/10.1029/2021MS002792>, 2022.

Ryu, Y.-H., Min, S.-K., and Knote, C.: Contrasting roles of clouds as a sink and source of aerosols: A quantitative assessment using WRF-Chem over East Asia, *Atmospheric Environment*, 277, 119073, <https://doi.org/10.1016/j.atmosenv.2022.119073>, 2022.

Samset, B. H., Myhre, G., Schulz, M., Balkanski, Y., Bauer, S., Berntsen, T. K., Bian, H., Bellouin, N., Diehl, T., Easter, R. C., Ghan, S. J., Iversen, T., Kinne, S., Kirkevåg, A., Lamarque, J.-F., Lin, G., Liu, X., Penner, J. E., Seland, Ø., Skeie, R. B., Stier, P., Takemura, T., Tsigaridis, K., and Zhang, K.: Black carbon vertical profiles strongly affect its radiative forcing uncertainty, *Atmospheric Chemistry and Physics*, 13, 2423–2434, <https://doi.org/10.5194/acp-13-2423-2013>, 2013.

Sapiano, M. R. P. and Arkin, P. A.: An Intercomparison and Validation of High-Resolution Satellite Precipitation Estimates with 3-Hourly Gauge Data, *Journal of Hydrometeorology*, 10, 149–166, <https://doi.org/10.1175/2008JHM1052.1>, 2009.

Seinfeld, J. H. and Pandis, S. N.: *Atmospheric Chemistry and Physics: From Air Pollution to Climate Change*, Third., John Wiley & Sons, Inc, New Jersey, 2016.

Shen, Z., Ming, Y., Horowitz, L. W., Ramaswamy, V., and Lin, M.: On the Seasonality of Arctic Black Carbon, *Journal of Climate*, 30, 4429–4441, <https://doi.org/10.1175/JCLI-D-16-0580.1>, 2017.

Slowik, J. G., Cross, E. S., Han, J.-H., Davidovits, P., Onasch, T. B., Jayne, J. T., Williams, L. R., Canagaratna, M. R., Worsnop, D. R., Chakrabarty, R. K., Moosmüller, H., Arnott, W. P., Schwarz, J. P., Gao, R.-S., Fahey, D. W., Kok, G. L., and Petzold, A.: An Inter-Comparison of Instruments Measuring Black Carbon Content of Soot Particles, *Aerosol Science and Technology*, 41, 295–314, <https://doi.org/10.1080/02786820701197078>, 2007.

Stahl, C., Crosbie, E., Bañaga, P. A., Betito, G., Braun, R. A., Cainglet, Z. M., Cambaliza, M. O., Cruz, M. T., Dado, J. M., Hilario, M. R. A., Leung, G. F., MacDonald, A. B., Magnaye, A. M., Reid, J., Robinson, C., Shook, M. A., Simpas, J. B., Visaga, S. M., Winstead, E., Ziemba, L., and Sorooshian, A.: Total organic carbon and the contribution from speciated organics in cloud water: airborne data analysis from the CAMP²Ex field campaign, *Atmospheric Chemistry and Physics*, 21, 14109–14129, <https://doi.org/10.5194/acp-21-14109-2021>, 2021.

Stein, A. F., Draxler, R. R., Rolph, G. D., Stunder, B. J. B., Cohen, M. D., and Ngan, F.: NOAA’s HYSPLIT Atmospheric Transport and Dispersion Modeling System, *Bull. Amer. Meteor. Soc.*, 96, 2059–2077, <https://doi.org/10.1175/BAMS-D-14-00110.1>, 2015.

Textor, C., Schulz, M., Guibert, S., Kinne, S., Balkanski, Y., Bauer, S., Berntsen, T., Berglen, T., Boucher, O., Chin, M., Dentener, F., Diehl, T., Easter, R., Feichter, H., Fillmore, D., Ghan, S., Ginoux, P., Gong, S., Grini, A., Hendricks, J., Horowitz, L., Huang, P., Isaksen, I., Iversen, I., Kloster, S., Koch, D., Kirkevåg, A., Kristjansson, J. E., Krol, M., Lauer, A., Lamarque, J. F.,



630 Liu, X., Montanaro, V., Myhre, G., Penner, J., Pitari, G., Reddy, S., Seland, Ø., Stier, P., Takemura, T., and Tie, X.: Analysis and quantification of the diversities of aerosol life cycles within AeroCom, *Atmospheric Chemistry and Physics*, 6, 1777–1813, <https://doi.org/10.5194/acp-6-1777-2006>, 2006.

Wang, J., Petersen, W. A., and Wolff, D. B.: Validation of Satellite-Based Precipitation Products from TRMM to GPM, *Remote Sensing*, 13, 1745, <https://doi.org/10.3390/rs13091745>, 2021a.

635 Wang, Y., You, Y., and Kulie, M.: Global Virga Precipitation Distribution Derived From Three Spaceborne Radars and Its Contribution to the False Radiometer Precipitation Detection, *Geophysical Research Letters*, 45, 4446–4455, <https://doi.org/10.1029/2018GL077891>, 2018.

Wang, Y., Xia, W., Liu, X., Xie, S., Lin, W., Tang, Q., Ma, H.-Y., Jiang, Y., Wang, B., and Zhang, G. J.: Disproportionate control on aerosol burden by light rain, *Nat. Geosci.*, 14, 72–76, <https://doi.org/10.1038/s41561-020-00675-z>, 2021b.

640 Wang, Y., Xia, W., and Zhang, G. J.: What rainfall rates are most important to wet removal of different aerosol types?, *Atmospheric Chemistry and Physics Discussions*, 1–33, <https://doi.org/10.5194/acp-2021-542>, 2021c.

Watson-Parris, D., Schutgens, N., Reddington, C., Pringle, K. J., Liu, D., Allan, J. D., Coe, H., Carslaw, K. S., and Stier, P.: In-situ constraints on the vertical distribution of global aerosol, *Aerosols/Atmospheric Modelling/Troposphere/Physics (physical properties and processes)*, <https://doi.org/10.5194/acp-2018-1337>, 2019.

645 Xu, D., Ge, B., Chen, X., Sun, Y., Cheng, N., Li, M., Pan, X., Ma, Z., Pan, Y., and Wang, Z.: Multi-method determination of the below-cloud wet scavenging coefficients of aerosols in Beijing, China, *Atmospheric Chemistry and Physics*, 19, 15569–15581, <https://doi.org/10.5194/acp-19-15569-2019>, 2019.

Xu, K.-M. and Randall, D. A.: A Semiempirical Cloudiness Parameterization for Use in Climate Models, *Journal of the Atmospheric Sciences*, 53, 3084–3102, [https://doi.org/10.1175/1520-0469\(1996\)053<3084:ASCPFU>2.0.CO;2](https://doi.org/10.1175/1520-0469(1996)053<3084:ASCPFU>2.0.CO;2), 1996.

650 Zhang, W., Huang, A., Zhou, Y., Yang, B., Fang, D., Zhang, L., and Wu, Y.: Diurnal cycle of precipitation over Fujian Province during the pre-summer rainy season in southern China, *Theor Appl Climatol*, 130, 993–1006, <https://doi.org/10.1007/s00704-016-1927-2>, 2017.

Zhao, X., Sun, Y., Zhao, C., and Jiang, H.: Impact of Precipitation with Different Intensity on PM_{2.5} over Typical Regions of China, *Atmosphere*, 11, 906, <https://doi.org/10.3390/atmos11090906>, 2020.

655



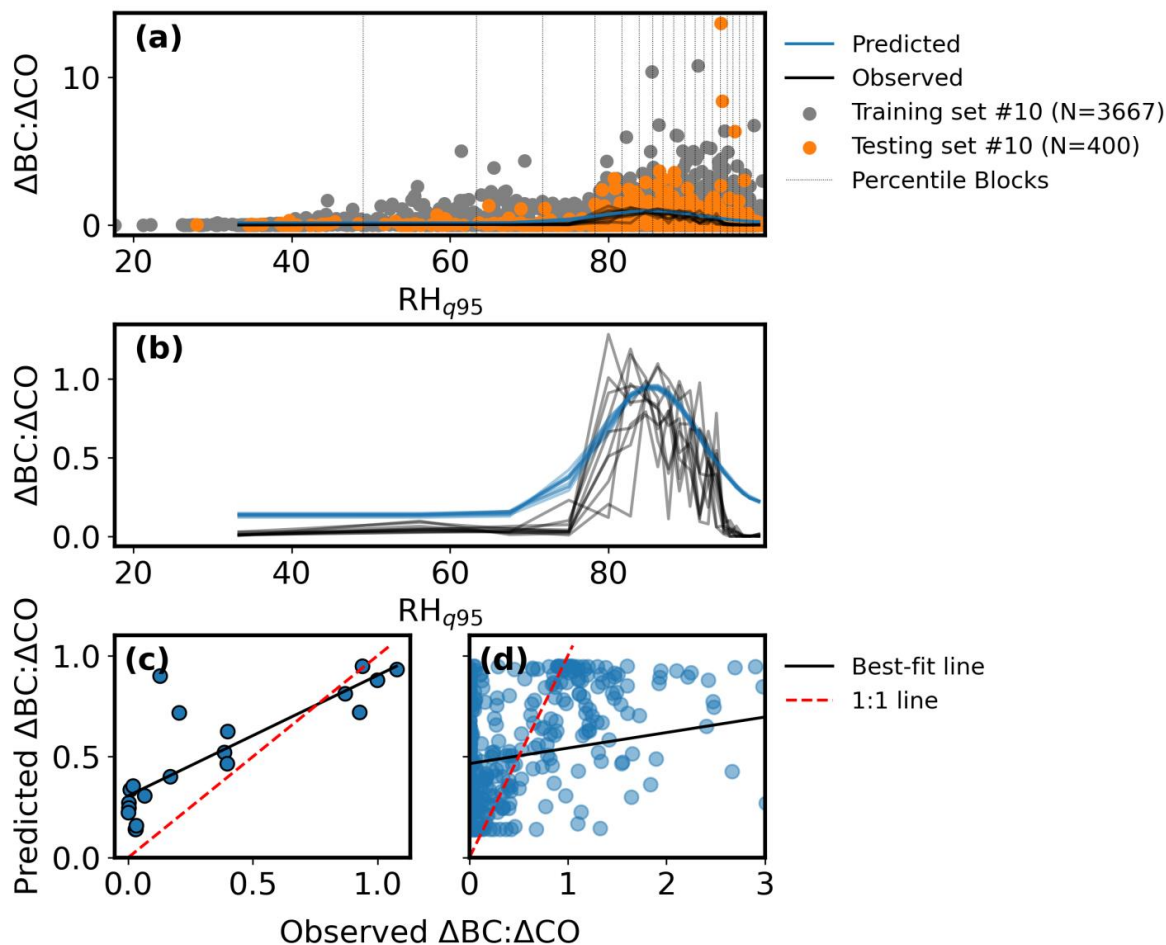
Table 1: Examples of notation used in this study.

Predictor	Description	Variations
f_{RH95}	Fraction of hours along trajectories where GFS relative humidity (RH) > 95%	f_{RH85} , f_{RH90}
f_{MR15}	Fraction of hours along trajectories where GFS water vapor mixing ratio (MR) > 15 g kg ⁻¹ dry air	f_{MR17}
RH_{q95}	95 th percentile of RH along trajectories	RH_{q50} , RH_{q85} , RH_{q90} , RH_{q100} , RH_{mean}
$RH_{w, DLH}$	RH over water measured by DLH onboard the aircraft	-
$APT_{PCP > 0.2 \text{ mm}, 48H, GFS, < 1500m}$	Accumulated precipitation calculated along 48-h trajectories where GFS precipitation is above 0.2 mm and trajectory altitude is below 1500 m	Trajectory duration: 12H, 24H, 48H, 72H Precipitation product: GFS, IMERG, PERSIANN-CDR Maximum altitude filter: no filter, < 1500 m Minimum precipitation filter: no filter, > 0.2 mm Other precipitation variables: PA, PF, PI

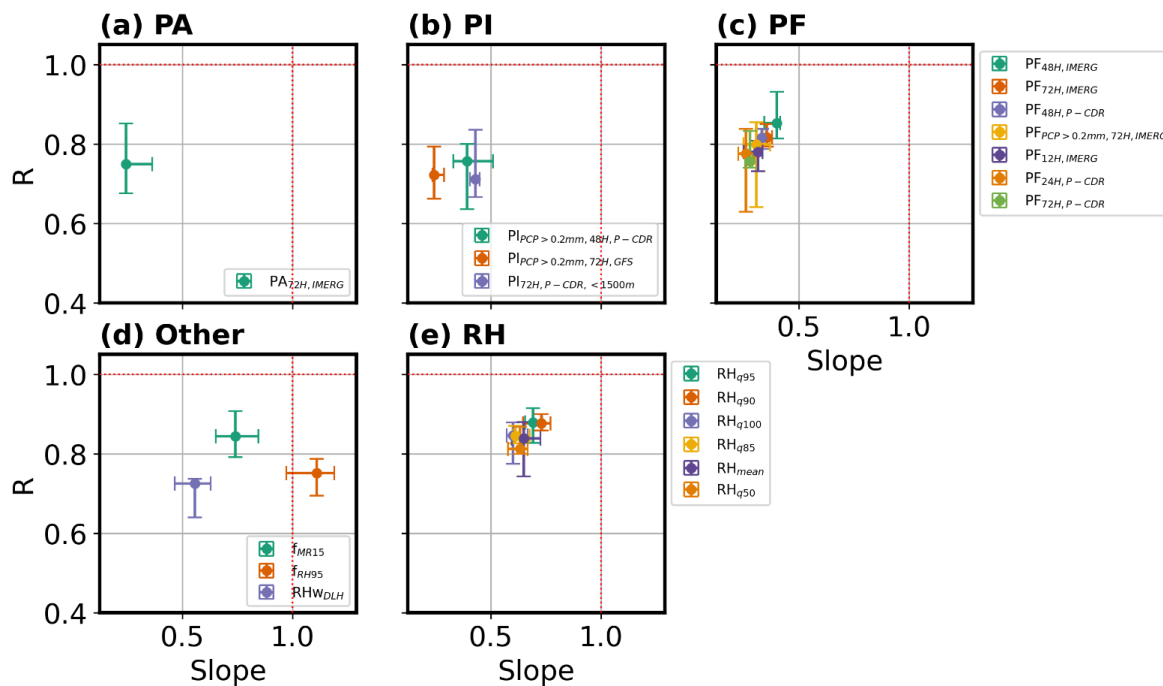


660 **Table 2: Curve-fitting equations considered where x is the predictor variable and y is the observed $\Delta BC/\Delta CO$ while a , b , c , and d are best-fit parameters determined via least-squares regression.**

Name	Equation	Source
Gaussian	$y = a \cdot \exp\left(-\frac{(x-b)^2}{2 \cdot c^2}\right) + d$	-
General Exponential	$y = a \cdot \exp(-b \cdot x) + c$	-
Oshima	$y = b - a \cdot \log_{10}(x)$	Oshima et al. (2012)
Kanaya	$y = c \cdot \exp(-a \cdot x^b)$	Kanaya et al. (2016)



665 **Figure 1:** An example of the curve-fitting procedure on $\Delta BC/\Delta CO$ with RH_{q95} as the predictor fitted with a gaussian function. (a) Training
 (gray dots) and testing sets (orange dots) for the 10th iteration of the k-fold cross-validation procedure selected using stratified random
 sampling. Percentile blocks are denoted by vertical gray lines with observed (black) and predicted curves (blue) also plotted for all 10
 iterations. (b) Same as (a) but only showing observed (black) and predicted curves (blue) for all 10 iterations to highlight variations
 between the k iterations. (c) Scatterplot comparing RH_{q95} -predicted $\Delta BC/\Delta CO$ and observed median $\Delta BC/\Delta CO$ per 5th percentile block
 of the predictor. Note that (c) is simply the linear regression of the observed and predicted curves in (b). (d) Same as (c) but comparing
 670 RH_{q95} -predicted and observed $\Delta BC/\Delta CO$ for individual points. In (c-d), only training set data are used, Y-axes are the same, the best-fit
 line is shown as a black line, and the 1:1 line is the red, dashed line.



675

Figure 2: Slope and Pearson correlation (R) values derived from linear regressions of observed (x) and predicted (y) $\Delta BC/\Delta CO$ with error bars representing the 25th and 75th percentile values derived from k -fold cross validation ($k=10$) using stratified random sampling (Sect. 2.5). Ideal values are denoted by the red dashed lines such that a better predictor would fall closer to the intersection of the two lines. Only predictors with median $R > 0.70$ are shown. Note that PERSIANN-CDR has been abbreviated to P-CDR (b-c). Panels share the same X- and Y-axis limits.

680

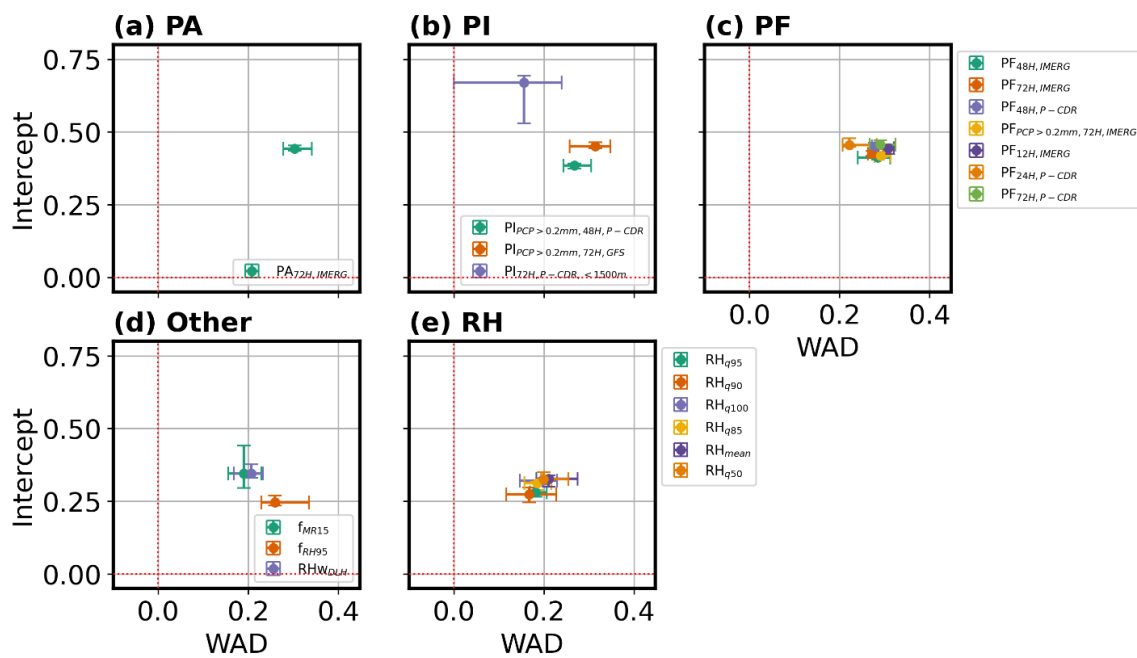
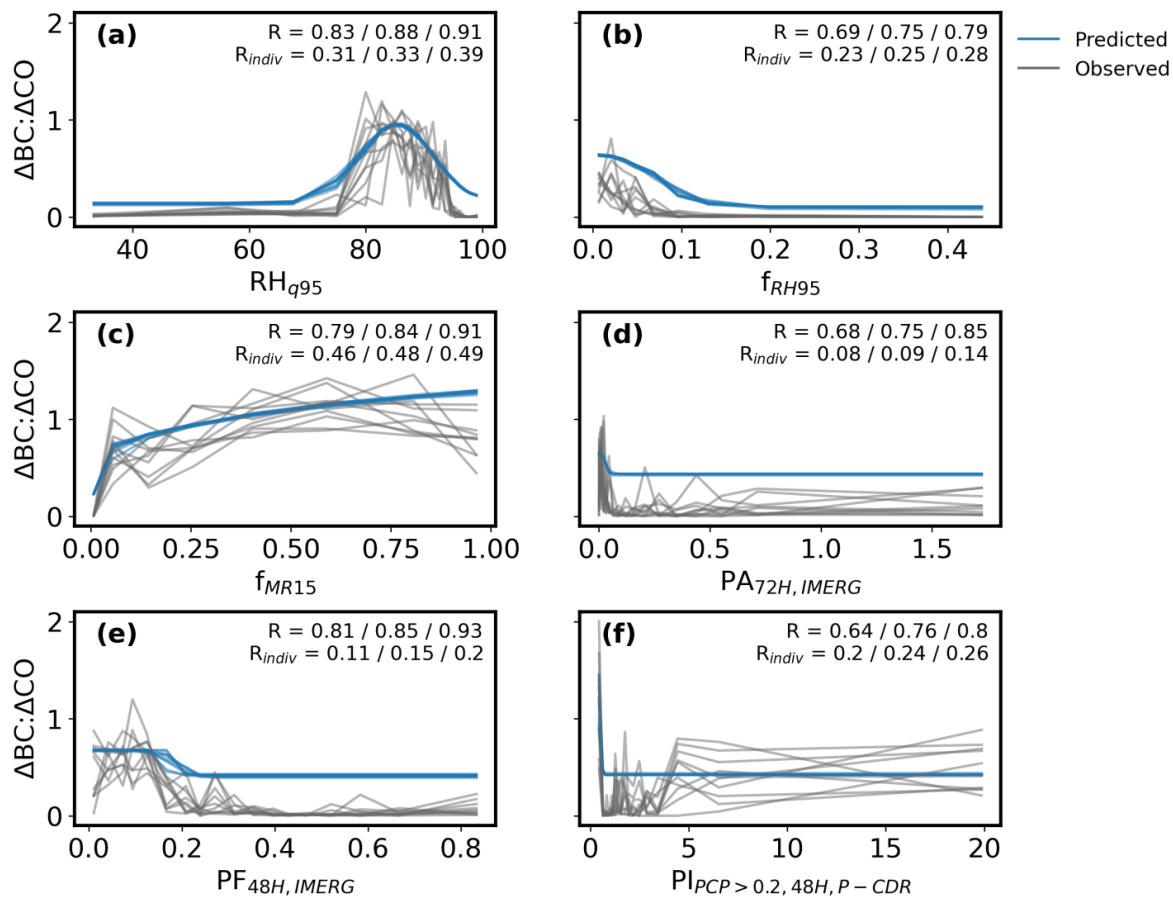


Figure 3: Same as Fig. 2 but comparing intercept and weighted area difference (WAD, Sect. 2.5).



685

Figure 4: Median values of observed (black) and predicted $\Delta ABC/\Delta CO$ (red) as a function of selected predictors for 10 iterations during k-fold cross-validation. Pearson correlations are annotated as 25th/50th/75th percentiles from k-fold iterations (k=10) calculated in two ways: comparing predicted and observed median $\Delta ABC/\Delta CO$ per 5th percentile block of the predictor (R) and comparing predicted and observed $\Delta ABC/\Delta CO$ for individual points (R_{indiv}). Panels share the same Y-axis limits.

690

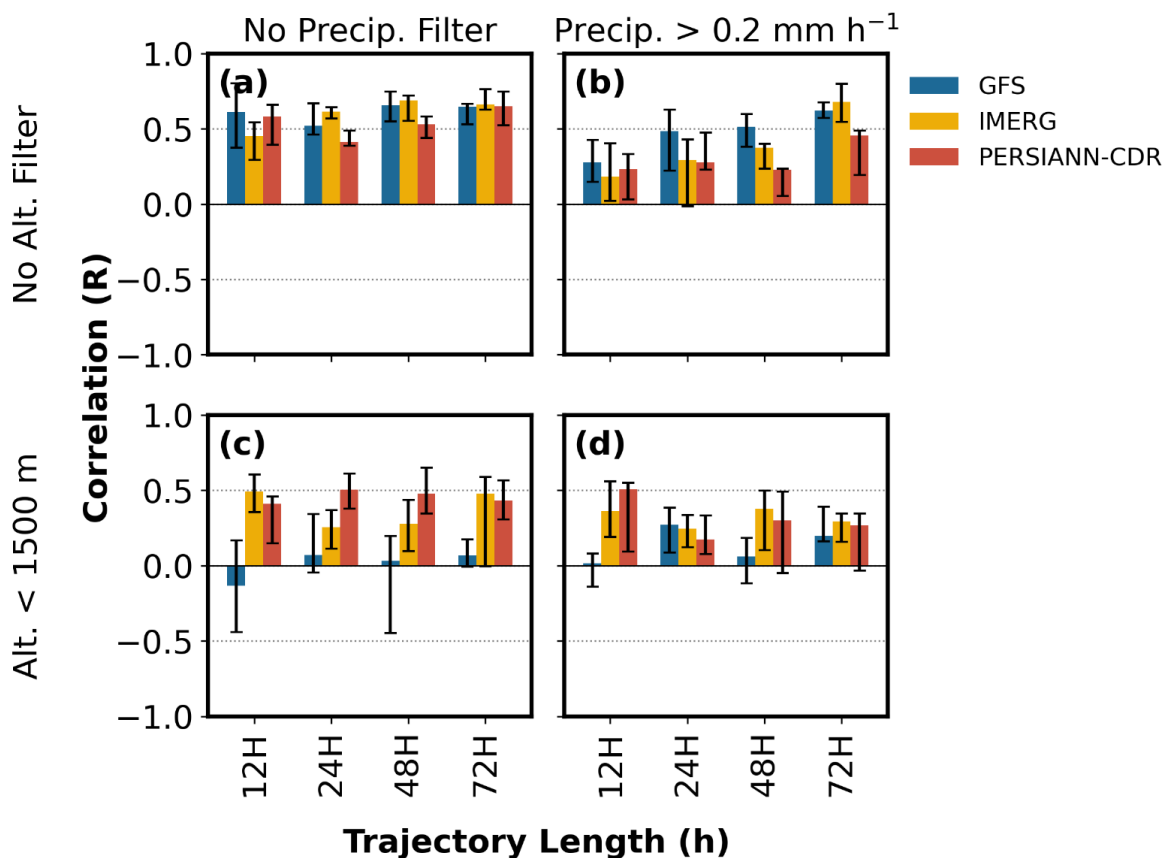


Figure 5: Pearson correlations (R) between observed $\Delta BC/\Delta CO$ and $\Delta BC/\Delta CO$ predicted by accumulated precipitation along trajectories (APT) for different trajectory lengths and precipitation data products. Each panel refers to a combination of altitude and precipitation intensity filters. Panels share the same X- and Y-axis limits.

695